Available online at www.sciencedirect.com
SCIENCE DIRECT®
International Journal of Thermal Sciences 44 (2005) 1110–1114
International Journal of Thermal Sciences
www.elsevier.com/locate/ijts

New cascades for thermo-chemical refrigeration

B. Spinner [b], M. Sorin [a,*], J. Berthiaud [b], N. Mazet [b], F. Rheault [a]

[a] *CANMET – CETC (Canadian Energy Technologies Center), 1615 Lionel-Boulet Boulevard, PO Box 4800, Varennes, PQ, Canada J3X 1S6*
[b] *PROMES (PROcédés, Matériaux et Energie Solaire), TECNOSUD – Rambla de la Thermodynamique, 66100 Perpignan, France*

Received 25 April 2005; accepted 8 September 2005

Available online 28 October 2005

Abstract

A diagrammatical approach for the design of new thermo-chemical cascades for heat management purposes is proposed. The two key elements of this approach are: a method to automatically generate system architectures and a general approach to selecting appropriate materials. It is based on establishing an explicit correspondence between the exergy balance around a thermo chemical system, the properties of the reactants and the operational system parameters. A new auto thermal configuration involving two thermally coupled single effect processes is proposed and suitable materials for its implementation are identified. The method is illustrated for the design of an experimental installation for the testing of a thermo-chemical refrigeration system operated at distance from a heat source.

Keywords: Exergy; Thermochemical process; Cascade system; Refrigeration; Waste heat

1. Introduction

Single effect systems based on solid–gas reactions have been demonstrated for heat pump, refrigeration and heat upgrading applications [1,2]. Such systems exhibit inherent storage capability and were also being investigated as heat transportation vector support [3–8], for example, to exploit a heat source located on one site to supply refrigeration needs at a distant site. Such attributes make solid–gas reactors attractive candidates for the management of heat from industrial wastes or renewable energy sources, which are generally low temperature, intermittent and require some distribution means between distant production and application sites. However, efficiency, safety or cost considerations often impose severe constraints on the temperature/pressure operational range, which, in turn, limit the number of gas–solid reaction candidates suitable for a specific application. Thermal cascade structures such as proposed by Alefeld and Radermacher [1] may be a valuable solution to overcome these limitations. In this paper, a thermodynamic diagrammatic approach is proposed for the development of innovative thermal cascade structures for the production of cold from a low/medium temperature heat source. This is a two-step approach. First, a method for generating appropriate thermal cascade structures of ideal processes is proposed. Then, general guidelines are given for the choice of suitable reactants. The method is applied to the structural design of an installation for the testing of a refrigeration system driven from a remote heat source.

2. Ideal single effect thermo-chemical refrigeration process and its representation with thermodynamic diagrams

The basic scheme of a single effect thermo-chemical refrigerator is shown in Fig. 1. Two reactors containing different solids or simply a solid reactor and a gas condenser/evaporator

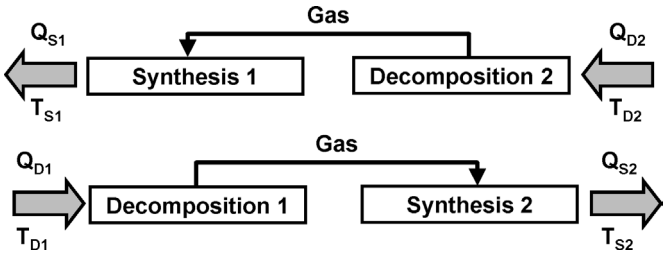

Fig. 1. A simple effect thermo-chemical refrigerator process.

* Corresponding author. Tel.: +1 (450) 652 3513; fax: +1 (450) 652 0999.
E-mail address: msorin@nrcan.gc.ca (M. Sorin).

1290-0729/$ – see front matter
doi:10.1016/j.ijthermalsci.2005.09.003

constitute the single effect refrigeration device. This is a two phase process, each involving two steps (s-synthesis, d-decomposition). In the cold production phase, at low pressure, solid 1 decomposes and gas flows to reactor 2, where it reacts with solid 2. As a result, the decomposition energy $Q_{D1} = \Delta H_{D1}$ (where ΔH_{D1} is the enthalpy variation due to the chemical reaction of decomposition) is extracted from the cold space at temperature T_{D1} and the heat of synthesis $Q_{S2} = \Delta H_{S2}$ is discarded by reactor 2 at temperature T_{S2}. In the regeneration phase, at higher pressure, the decomposition of solid 2 requires a heat input $Q_{D2} = \Delta H_{D2}$ from the heat source at temperature T_{D2}. The gas produced is directed to reactor 1 where the heat of synthesis $Q_{S1} = \Delta H_{S1}$ is discarded at temperature T_{S1}. The selection of reactive solids allows adjusting the temperature and pressure conditions to the process constraints.

As presented by Sorin et al. [9], the operation of an ideal single effect thermo-chemical refrigerator may be represented on a Carnot factor, ($\theta = 1 - T_0/T$) vs. heat (Q) diagram (T_0 is the environment temperature) further referred to as a θ–Q diagram. A particular case where $\theta_{S1} = \theta_{S2} = \theta_0 = 0$ is illustrated in Fig. 2(a). The driven heat flow Q_{D1} is upgraded from θ_{D1} to θ_0 due to the driving heat flow Q_{D2}, which degrades from θ_{D2} to θ_0. The rectangular areas associated with the driven and driving heat flows represent respectively the exergy of the produced cold and the expended exergy of the input heat. For an ideal system, they are equal. Furthermore, for system analysis considerations [9,10], it is convenient to split each $Q = \Delta H$ value in two terms: the latent heat necessary to evaporate or condense the gas (l) and the remainder part $r = Q - l$. Heat (l) is the internal energy transport vector while heat (r) is stored within the solid during the decomposition process and released out of the system during the synthesis process. Fig. 2(a) illustrates the exergy variation due to the temperature changes associated with each energy component (l or r_i) involved in the device and shown in Fig. 1. For further reference, each rectangular area is called an exergy dipole. There are four dipoles of two different types: those labeled by up going arrows and named uphill dipoles and those labeled by down going arrows and named downhill dipoles.

The correspondence between the θ–Q diagram and the Clausius–Clapeyron diagram was noted by Sorin et al. [10]. Here, this correspondence is made more explicit by expressing the Clausius–Clapeyron as a function of the Carnot factor θ i.e. $\ln p = \Delta H\theta/RT_0 +$ constant as illustrated in Fig. 2(b). This diagrammatic representation provides a convenient method to link exergy balance design considerations and the thermo-chemical properties of the reactants to the operational conditions of the system.

For the sake of simplicity, here, it is assumed that all dipoles in Fig. 2(a) have the same width (energy $r_1 = r_2 = l$) so that the corresponding gas–solid equilibrium lines in the θ–$\ln p$ diagram are parallel.

In practice, there exist a limited number of solid–gas reactions and it is unlikely that a single effect thermo-chemical process will satisfy all the temperature and pressure constraints, especially for systems involving transport at distance between two sites, a feature that may impose severe material constraints due to efficiency and safety considerations. In this regard, new thermal cascade structures made out of thermally coupled single effect thermo chemical processes are proposed. The intent is to have each single effect process to meet only a subset of the constraints so as to improve the likelihood of identifying adequate gas–solid reactions.

3. Technique for cascade structure design

In gas solid reactions, the path of the energy transported by the gas necessarily tracks the unfolding of the process. Thus, for thermal cascade structure design purposes, it is only necessary to devise new gas energy paths to automatically generate new system structures. The intent, here, is to design such structures in view of extending the temperature dynamic range of the energy currents (l) within the thermo-chemical cycle. In this simplified representation, a single effect gas–solid reaction is represented by a set of one uphill and one downhill dipole as shown in Fig. 3(a). The thermally coupled reactors, otherwise called "auto-thermal reactors", are described by a set of two "compensated dipoles" having a common temperature. Each compensated dipole illustrated in Fig. 3(b) is an assembly of uphill and downhill dipoles linked together by an arrow representing the heat recovery. There are several ways to combine such compensated dipole sets with the basic dipoles of Fig. 3, each corresponding to a different system structure. One

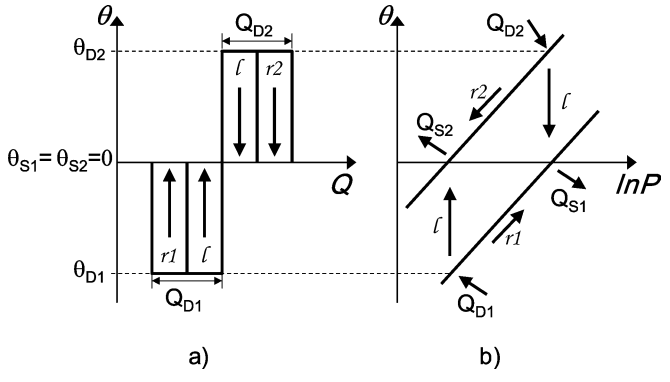

Fig. 2. (a) Exergy dipole representation on the Carnot factor–heat diagram, and (b) the corresponding representation on a Carnot factor–ln p diagram.

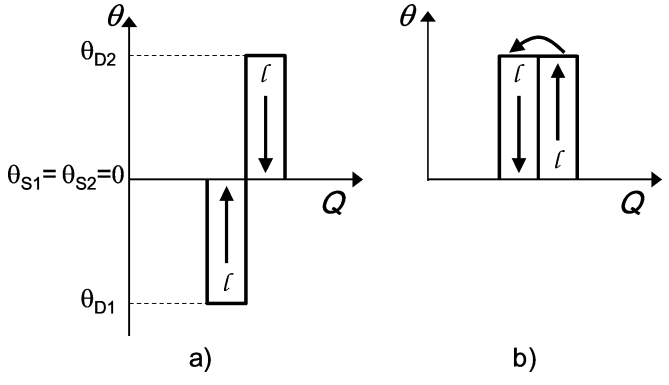

Fig. 3. Single effect exergy dipoles (a), and compensated dipole (b), associated with gas transfer in the Carnot factor–heat diagram.

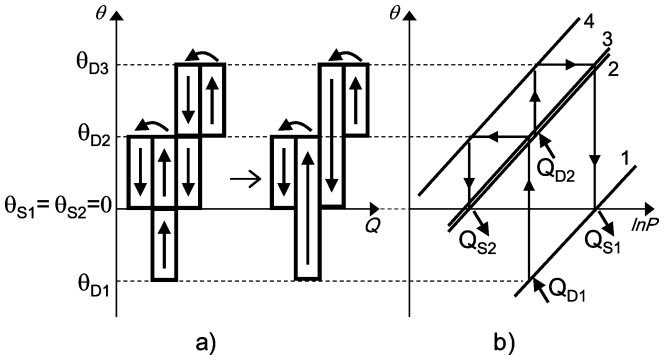

Fig. 4. (a) Dipole combination involving a compensated dipole placed above the uphill and downhill dipoles with heat recovery taking place above T_0. (b) A thermo-chemical cascade using three pressure levels.

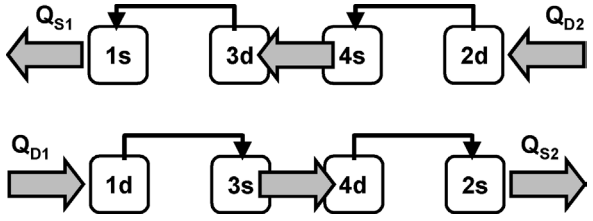

Fig. 5. Architecture of a cascade with heat recovery above T_0 (same symbol as in Fig. 1).

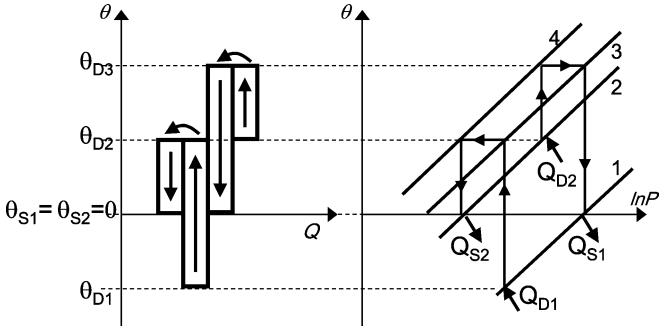

Fig. 6. A thermo-chemical cascade with four pressure levels and heat recovery above T_0 on: (a) Carnot factor–heat diagram, (b) Carnot factor–ln p diagram.

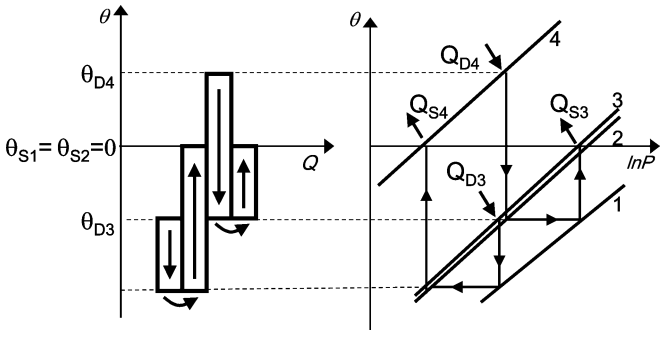

Fig. 7. (a) Dipole combination involving A compensated dipole placed bellow the uphill and downhill dipoles. (b) A thermo-chemical cascade using three pressure levels.

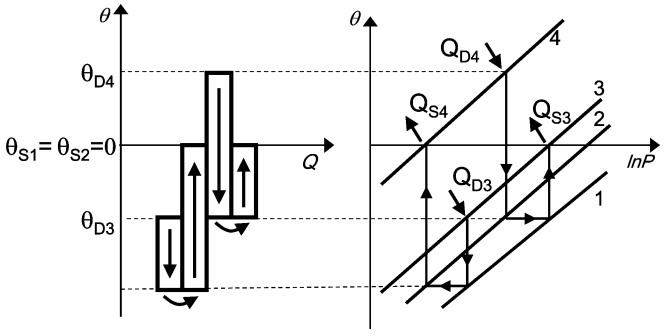

Fig. 8. A thermo-chemical cascade using four pressure levels and heat recovery bellow T_0 on: (a) Carnot factor–heat diagram, (b) Carnot factor–ln p diagram.

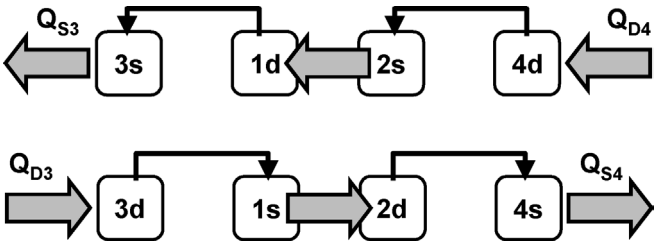

Fig. 9. The architecture of a cascade with heat recovery below T_0 (same symbol as in Fig. 1).

of the possible configuration is presented in Fig. 4(a). The compensated dipoles are placed just above the uphill and downhill dipoles. The graphical correspondence between the presentation in Fig. 4(a) and the θ–ln p diagram depends upon the number of pressure levels. For example Fig. 4(b) illustrates a cascade of thermo-chemical processes using three pressure levels. The equilibrium lines 2 and 3 are the same. The difference in the numbering only emphasizes the fact that there are two different reactors 2 and 3 containing the same reacting solid. The architecture of the cascade is automatically derived from Fig. 4(b) and is presented in Fig. 5. The net result is that the heat source at a given intermediate temperature generates heat at a higher level suitable to drive a second reaction and, thus, offer more flexibility in the choice of materials.

The procedure to design a four pressure level cascade is illustrated in Fig. 6. The architecture of this cascade is the same as in the previous case but this configuration opens the possibility of using different gas in each section of the thermal cascade.

Obviously the same procedure may be applied to build cascades with more than four pressure levels. It requires more equilibrium lines in the θ–ln p diagram and, as a result, more reactants are needed. Fig. 7 for three pressure levels and Fig. 8 for four pressure levels illustrate another structure where compensated dipoles are placed below the uphill and downhill dipoles. Contrary to the previous cases, the heat recovery takes place in the temperature region below θ_0. The architecture of these cascades is presented in Fig. 9. It is similar to the one presented in Fig. 5, however the sequence of reactions is different.

The general approach for choosing the reactants is an iterative process. Referring to Fig. 5, one can see that the available heat source, the required refrigeration and available sink temperatures determine the operating temperatures of the reactors in contact with the source and with the cold space. So, θ_{D2}, θ_{D1}, θ_{S2}, and θ_{S1} in Fig. 6 are uniquely determined. Then, out of a list of potential candidates, one can pick reactants that satisfy the pressure constraints, which are imposed on the cor-

responding portion of the cascade. This choice, in turn, also determines the operating pressures of the gases in the corresponding auto thermal reactors. Since the auto thermal reactors are in thermal contact, their temperature in the production and the regeneration phases are equal so that $\theta_{D3} = \theta_{S4}$ and $\theta_{D4} = \theta_{S3}$. For the case shown in Fig. 6, these temperatures are not fixed but they must be larger than the heat source and satisfy any other imposed constraints. The final choice of the auto thermal reactants involves picking one reactant that satisfies the above pressure/temperature conditions out of the potential candidate list and verifying how close the other reactants satisfy the corresponding conditions for the other auto thermal reactor. The process is iterated for all candidates to find the combination of auto thermal reactants that presents the best fit.

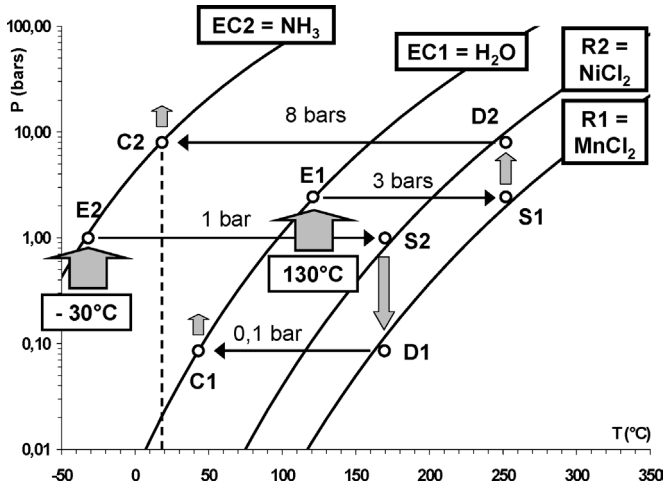

Fig. 10. Example of cold production using two gas–liquid and two gas–solid equilibrium lines.

4. Case study

In spite of the fact that there exist a large number of solid–gas reactions, one cannot easily identify a suitable pair of such reactions to design a single effect system that will meet all the constraints of a given application. In fact, in most applications, the source, sink and usage temperatures are all fixed. This, in turn, completely determines the operational conditions of a single effect solid–gas reactor. Failure of having a match between the set application temperatures and the operating point of the reactants results in a loss of exergy. Considering that additional constraints on the gas pressure range are often imposed for efficiency, safety or durability considerations, makes it still more difficult, if possible at all, to identify suitable materials. Making use of the thermal cascade approach offers more flexibility on the choice of the materials.

Its application is demonstrated in Fig. 10 for the preliminary design of an experimental installation to study the performance of a refrigeration system at $-30\,^{\circ}\mathrm{C}$ driven by a heat source at $130\,^{\circ}\mathrm{C}$ and located in a remote site. The following nomenclature is used in Fig. 10: *E*-evaporation, *C*-condensation, *D*-decomposition and *S*-synthesis. The heat sink at both sites is the environment at $20\,^{\circ}\mathrm{C}$. The pressure of the transport gas has to be constrained between 1 and 10 bars while the pressure in the other section should be confined to the 0.05 to 10 bars range. Furthermore, for reliability considerations, only well proven gas–solid reactions are to be used, so that out of a few hundred available reactants, only a dozen ammonia salts and hydrates were considered. In these conditions, only an ammonia condenser/evaporator can be used at the refrigeration site, thus imposing ammonia as a transport agent. Similarly, a water condenser/evaporator receives energy from the source at $130\,^{\circ}\mathrm{C}$ and boils water at a pressure of 3 bars. The auto-thermal reactor then consists of two thermally coupled reactors filled with a hydrate and ammonia salt. For material stability considerations, the maximum temperature of the auto-thermal reactor is set at $350\,^{\circ}\mathrm{C}$. Using the method described previously, $MnCl_2/H_2O$ and $NiCl_2/NH_3$ were selected. In the regeneration phase, the heat source boils water at $130\,^{\circ}\mathrm{C}$, which reacts with $MnCl_2/H_2O$ to produce heat at $250\,^{\circ}\mathrm{C}$ in the auto-thermal reactor. This energy is transferred to decompose the $NiCl_2/NH_3$ salt. The NH_3 heat of condensation is then discarded in the environment at $20\,^{\circ}\mathrm{C}$. In the production phase, the evaporation of the ammonia draws heat from the cold space at $-30\,^{\circ}\mathrm{C}$ and flows to the auto-thermal reactor where it reacts with the $NiCl_2/NH_3$ salt to supply decomposition heat to the $MnCl_2/H_2O$ salt. Water condenses at a pressure of 0.1 bar and heat is discarded at $40\,^{\circ}\mathrm{C}$ in the environment, thus experiencing a small temperature mismatch.

Although this example only addresses the design of a simple ideal process, it clearly illustrates the application of the method. It emphasizes one of the interest of assembling two different fluids in such an integrated process: the higher pressure gas (ammonia) is used at low temperature, while the lower pressure gas (water) is used at higher temperature, allowing the integrated process to fulfill simultaneously both the temperature and pressure constraints.

The identification of adequate materials in real systems would follow the same basic procedure, due account being given to the heat and mass transfer exergy losses.

5. Conclusion

This paper describes a diagrammatic design method that explicitly makes use of the correspondence between thermodynamic design considerations, the thermo-chemical properties of the reactants and the operational parameters of the system. It involves a two step procedure whereby a suitable system configuration is first identified out of an automatically generated set of structures. In a second step, available reaction data bases are scanned for the selection of materials that allow meeting operational constraints. The method is illustrated for the design of a thermo chemical refrigeration system. It shows how an application for which a suitable single effect reaction is not available could be implemented using the thermal cascade approach. It could equally well be applied to the design of heat pump or heat upgrading processes.

Only thermo-chemical reactions involving ammonia salts and hydrates were considered here but the thermal cascade ap-

proach lends itself to using other types of reaction such as hydrides and carbonates thus considerably enlarging the scope of gas–solid candidates and the variety of applications. Finally, only ideal systems were considered but accounting for exergy losses due to heat and mass transfer in the design of real systems would basically follow the same procedure. In all, it is believed that the method proposed here may prove to be a very valuable asset for the design of real systems for waste heat or renewable energy valorization processes.

References

[1] G. Alefeld, R. Radermacher, Heat Conversion Systems, CRC Press, Boca Raton, FL, 1994.
[2] V. Goetz, F. Elie, B. Spinner, The structure and performance of single effect solid–gas chemical heat pumps, Heat Recovery Systems & CHP 13 (1) (1993) 79–96.
[3] G. Alefeld, Vorschlag für ein Fernwärmeversorgungssystem, Brennstoff-Wärme-Kraft 28 (1) (1976) 12–18.
[4] P.W. Bach, W.G. Haije, Storage, transformation and transport of heat along the thermochemical route, presented at IEA-Annex 10 (Phase change materials and chemical reactions for thermal energy storage), Adana, Turkey, April 16–17, 1998.
[5] K. Nasako, Y. Ito, M. Osumi, Intermittent heat transport using hydrogen absorbing alloys, Int. J. Hydrogen Energy 23 (9) (1998) 815–824.
[6] H. Hasegawa, H. Ishitani, R. Matsuhashi, M. Yoshioka, Analysis on waste-heat transportation systems with different heat-energy carriers, Appl. Energy 61 (1998) 1–12.
[7] Y.T. Kang, A. Akisawa, Y. Sambe, T. Kashiwagi, Absorption heat pump systems for solution transportation at ambient temperature—STA cycle, Energy 25 (4) (2000) 355–370.
[8] B. Spinner, N. Mazet, D. Stitou, New sorption cycles for heat and/or cold production adapted for long distance heat transmission, in: ASME International Mechanical Engineering Congress, New Orleans, 2002.
[9] M. Sorin, B. Spinner, D. Stitou, Synthesis of single effect solid–gas thermochemical refrigerators, in: Proceedings of Trans IchemE, vol. 78, Part A, 2000, pp. 795–802.
[10] M. Sorin, B. Spinner, D. Stitou, Thermodynamic techniques for the conceptual design of thermochemical refrigerators using two salt materials, Chem. Engrg. Sci. 57 (2002) 4243–4251.